

PHASE-BASED DETECTION OF INTENTIONAL STATE FOR ASYNCHRONOUS BRAIN-COMPUTER INTERFACE

Kaori Suefusa and Toshihisa Tanaka

Department of Electrical and Electronic Engineering,
Tokyo University of Agriculture and Technology
Nakacho, Koganei-shi, Tokyo, 184-8588, Japan
Email: suefusa@sip.tuat.ac.jp, tanakat@cc.tuat.ac.jp

ABSTRACT

An asynchronous brain-computer interface (BCI) is one of the crucial challenges in biomedical signal processing. In asynchronous BCIs, a state when a user does not intend to input commands needs to be distinguished from a state when he/she does. These states are called non-control (NC) state and intentional control (IC) state respectively. In this paper, a new phase-based method to discriminate between IC/NC states for steady-state visual evoked potential (SSVEP) based asynchronous BCIs is proposed. The method has a two-step tree structure: in the first step, a SSVEP frequency is recognized with canonical correlation analysis (CCA), and in the next step, the state of a user is detected as IC or NC with a classifier such as SVM using phase information. The proposed method was tested on six healthy subjects and has been proved to be reliable in terms of sensitivity and specificity.

Index Terms— Brain-computer interface, Asynchronous BCI, Steady-state visual evoked potentials, Phase locking value, Support vector machine

1. INTRODUCTION

Brain-computer interfacing (BCI) is an emerging and potential application of signal processing and machine learning in human computer interaction. BCI controls a computer or a device by capturing human brain activities [1]. This technology provides another way of communication for people who have difficulty in communicating with the external world [2].

A well-known noninvasive recording of the brain activity is electroencephalogram (EEG). Typical responses of the brain are steady-state visual evoked potentials (SSVEPs), which are responses of the visual cortex to a periodic visual stimulus such as flickering lights [3], event related potentials (ERPs), which are responses to sensory or cognitive event [4], and so forth. Among them, SSVEP allows BCIs to achieve fast and accurate command input, and various BCIs based on SSVEP have been reported [5–15].

BCIs can be divided into synchronous and asynchronous ones by its operational protocol [5, 8]. With the synchronous BCIs, a timing of command input is controlled by the BCI and operations are executed with a certain time interval. However, in a real environment, not all the time a user intends to input commands. On the other hand, with the asynchronous BCIs, the user can input a command

when he/she intends to do so. Thus the asynchronous BCIs are considered to be a promising component of practical BCIs that require asynchronous operational protocol [5, 9]. In the asynchronous BCIs, a state when the user does not intend to input commands needs to be considered. This state is typically called non-control (NC) state while a state when the user intends to input commands is called intentional control (IC) state [5, 6, 9, 10, 16].

Recently, Cecotti [6] has proposed a self-paced and calibration-less BCI speller based on SSVEP. Also, Parini *et al.* [7] have presented a self-paced SSVEP-BCI using the common spatial patterns (CSPs) to spatially filter the signal derived from each channel. Their methods were highly focused on boosting the recognition accuracy and the information transfer rates (ITRs). Meanwhile, the subjects were constantly in the IC state and the NC state was not considered in their experimental paradigm. Besides, Xia *et al.* [5] have proposed a method for discrimination between the IC and the NC states based on the canonical correlations, and the performance was evaluated in the online asynchronous paradigm. Although, in the asynchronous experiment, it needed at least 5.0 seconds to input one command and the performance got worse with a shorter period of time to input it.

In this paper, we propose a new method of discrimination between the IC and the NC states for an asynchronous SSVEP based BCI. This method has a two-step tree structure as follows: in the first step, a frequency of visual stimulus is estimated with canonical correlation analysis (CCA). In the second step, IC/NC states are classified with SVM using phase locking value (PLV) as features. The recorded EEG in our experiment was analyzed offline and the performance was compared with a previous method.

2. METHODS

2.1. Subjects and experimental settings

Five males and one female in their twenties took part in our experiment. All subjects were healthy and had normal or corrected-to-normal vision. They were given an informed consent, and this study was approved by the research ethics committee of Tokyo University of Agriculture and Technology.

We used Ag/AgCl active electrodes which are products of Guger Technologies (g.tec) named g.LADYbird, g.LADYbirdGND (for GND), and g.GAMMAearclip (for reference, earclip type) for recording EEG data. These were driven by the power supply unit named g.GAMMAbox (g.tec). The electrodes were located at Pz, POz, Oz, O1 and O2 following the international 10–20 system [17]. The electrodes for GND and reference were AFz and A1, respectively. The signals were amplified by MEG-6116 (Nihon Kohden),

This work is supported in part by JSPS KAKENHI Grant Number 24360146. Toshihisa Tanaka is also affiliated with RIKEN Brain Science Institute, Saitama, Japan.

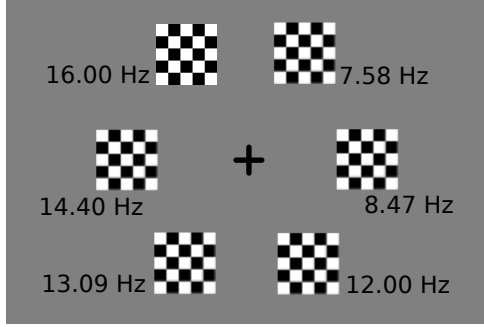


Fig. 1. An image of displayed targets. Each target was flickered with different frequencies as visual stimuli. A centered cross was a cue for trials of the NC state.

Table 1. Flickering frequencies assigned to BCI commands corresponding to visual targets on the screen.

Target T_k	Frequency f_k
T1	7.58 Hz
T2	8.47 Hz
T3	12.00 Hz
T4	13.09 Hz
T5	14.40 Hz
T6	16.00 Hz

that provides lowpass and highpass analog filters for each channel. We set the cutoff frequencies of the lowpass and the highpass filters to 100 Hz and 0.5 Hz, respectively. The EEG signal was sampled by A/D converter (AIO-163202F-PE, Contec) with a sampling rate of 1,440 Hz. The signals were recorded and downsampled to 240 Hz with Data Acquisition Toolbox of the MATLAB (MathWorks).

Fig. 1 shows an image of displayed targets. As illustrated in Fig. 1, six targets as visual stimuli were displayed on a 24 inch LCD monitor with a resolution of 1920×1080 and a refresh rate of 144 Hz. The targets were square checkerboards that reversed black and white according to the frequencies listed in Table 1. In the experiment, the subjects seated on a comfortable chair in front of a display 55 cm away so that they could look at the display straight ahead.

2.2. Task

In IC trials, the subjects gazed at one of the flickering targets, and in NC trials, the subjects gazed at the non-flickering centered cross as illustrated in Fig. 1. The subjects performed each IC/NC trial alternatively. Each trial lasted 3 seconds. Each session was consisted of 20 successive trials and five sessions were executed for each subject. After each session, the task was stopped in order to reduce the fatigue of the subjects' eyes.

2.3. Data analysis

Recorded EEG in the experiment were analyzed offline. As illustrated in Fig. 2, our proposed method has two steps:

Step 1. Detect the potential frequency with CCA,

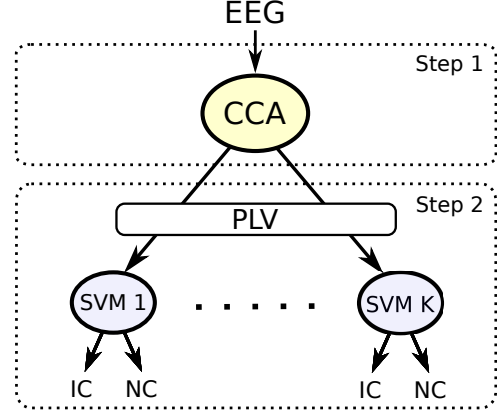


Fig. 2. The proposed decision tree. In the first step, the CCA identifies the frequency that may correspond to the SSVEP. In the second step, the SVM with respect to each target frequency is used as a classifier to determine whether the frequency component is the SSVEP response, that is, IC or NC state.

Step 2. Classify a feature vector consisting of the PLVs at all channels with SVM to discriminate between the IC and the NC states.

In addition, we ignored samples corresponding to 0.15 seconds just after a trial started considering a delay of SSVEP onset [18]. Thus, the signal for $3 - 0.15 = 2.85$ seconds was used for the analysis.

The underlying idea behind this two-step method is as follows: in the IC state, EEG signal would be in phase with a signal with a SSVEP frequency. On the other hand, in the NC state, there would be no SSVEP, thereby EEG signal would be out of phase. For this reason, the phase synchrony of the IC state is expected to be greater than that of the NC state. Accordingly, we can discriminate those states measuring the phase synchrony as the PLV.

2.3.1. Detection of the stimulus frequency with CCA

In the first step, the SSVEP frequency was detected by applying CCA. Let $\mathbf{x}(t) \in \mathbb{R}^M$ be an M -channel EEG signal and $\mathbf{y}(t) \in \mathbb{R}^{46}$ consist of 'Fourier basis functions' of the 1st and 2nd harmonics of simulated stimulus signals, which are ideal SSVEP with frequency f given as

$$\mathbf{y}(t) = [\{\sin(2\pi ft), \cos(2\pi ft), \sin(4\pi ft), \cos(4\pi ft)\}_{f \in \Omega}]^T, \quad (1)$$

where the first two components are the sinusoids of the fundamental frequency f , the others are the 2nd harmonics, and Ω is the set of frequencies as listed in Table 1. To detect frequencies of SSVEP components contained in the EEG for the SSVEP-based BCI systems, first, canonical correlation ρ corresponding to flickering frequency f is calculated:

$$\rho = \max_{\mathbf{w}_x, \mathbf{w}_y} \frac{\mathbf{w}_x^T E[\mathbf{x}(t)\mathbf{y}^T(t)]\mathbf{w}_y}{\sqrt{\mathbf{w}_x^T E[\mathbf{x}(t)\mathbf{x}^T(t)]\mathbf{w}_x \mathbf{w}_y^T E[\mathbf{y}(t)\mathbf{y}^T(t)]\mathbf{w}_y}}. \quad (2)$$

Then, frequency \hat{f} that maximizes the weight vector with respect to $\mathbf{y}(t)$ is chosen, that is,

$$\hat{f} = \operatorname{argmax}_{f \in \Omega} \left[(w_f^s)^2 + (w_f^c)^2 + (w_{2f}^s)^2 + (w_{2f}^c)^2 \right], \quad (3)$$

where w_f^s , w_f^c , w_{2f}^s and w_{2f}^c are the elements in the weight vector given as in

$$\mathbf{w}_y = \left[\left\{ w_f^s, w_f^c, w_{2f}^s, w_{2f}^c \right\}_{f \in \Omega} \right]^T, \quad (4)$$

which is the solution of (2).

It is worth noting that our method is based on the method proposed by Kimura *et al.* [19] that employed the weight vector with respect to $\mathbf{y}(t)$ to select the stimulus frequency as described in (3). This method uses a reference vector including sinusoids of all target frequencies. Thus, we carry out the CCA only once. On the other hand, Lin *et al.*'s method [20] should apply the CCA K times, the number of flicking patterns. For further details about their methods, see [19, 20].

2.3.2. Discrimination between the IC and the NC state

In the next step, we determined whether the stimulus frequency \hat{f} detected above was derived from SSVEP or not based on phase information called phase locking value (PLV) as features to be classified.

The PLV is widely used to measure phase synchronization of two signals by the instantaneous phase difference [21–23]. It is defined as follows:

$$\text{PLV}_{m,h} = \left| \langle e^{j\Delta\phi_{m,h}(t)} \rangle \right|, \quad (5)$$

with

$$\Delta\phi_{m,h}(t) = \phi_{y_h}(t) - \phi_{x_m}(t), \quad (6)$$

where $\phi_{x_m}(t)$ is instantaneous phase of $x(t)$ at channel m , $\phi_{y_h}(t)$ is instantaneous phase of $y(t)$ with the h th harmonic of a frequency, and $\langle \cdot \rangle$ is the averaging operator over time. We used the samples for the CCA to calculate the PLV, so that the averaging operator takes the average over 2.85 seconds ($2.85 \times 240 = 684$ samples). Besides, we calculated the PLV between an EEG signal $x_m(t)$ and a reference complex signal with the estimated stimulus frequency \hat{f} as

$$y_h(t) = \exp(2\pi\hat{f}ht), \quad (7)$$

where h denotes an order of harmonic. Here, we set the order of harmonic as $h = 1, 2$ as described before. The PLV of \hat{f} and its 2nd harmonic at each channel was calculated to construct one feature vector as

$$\mathbf{u} = [\text{PLV}_{1,1}, \dots, \text{PLV}_{M,1}, \text{PLV}_{1,2}, \dots, \text{PLV}_{M,2}], \quad (8)$$

where M is again the number of channels. Thus, the size of \mathbf{u} in the method is $5 \times 2 = 10$. To calculate the PLV, the instantaneous phase of the signal needs to be estimated. The PLV calculated for each channel and each harmonic was used for features to discriminate between the IC and the NC states with support vector machine (SVM) using linear kernel and the penalty parameter $c = 1$. We employed three methods to extract the phase: continuous wavelet transform (CWT), Hilbert transform (HT) and discrete Fourier transform (DFT) as described below.

A. Continuous wavelet transform

Wavelet analysis gives us a flexible way to analyze nonstationary signals such as EEG [24]. The CWT of a signal $x(t)$ is given as [25]

$$W(a, b) = \frac{1}{\sqrt{a}} \int_{-\infty}^{\infty} x(t) \psi^* \left(\frac{t-b}{a} \right), \quad (9)$$

where $\psi^*(\cdot)$ is the complex conjugate of the scaled and shifted mother wavelet, a is the scale factor and b is the shift factor. In this

paper, the complex Morlet wavelet was used as mother wavelet, which is often used in EEG analysis [26, 27] defined as follows [25]:

$$\psi(t) = \frac{1}{\sqrt{\pi f_b}} e^{i2\pi f_c t} e^{-\frac{t^2}{f_b}}, \quad (10)$$

where $f_b = 1.0$ is the bandwidth parameter, $f_c = 1.0$ is the wavelet center frequency and $i = \sqrt{-1}$ is the imaginary unit. Thus, the instantaneous phase can be determined with the wavelet coefficients as

$$\phi(a, b) = \arctan \left(\frac{\Im(W(a, b))}{\Re(W(a, b))} \right), \quad (11)$$

where $\Re(\cdot)$ denotes the real part and $\Im(\cdot)$ denotes the imaginary part.

B. Hilbert transform

The HT also allows us to extract the instantaneous phase [28] of a narrowband signal. The HT of a signal $x(t)$ is given as

$$\tilde{x}(t) = \frac{1}{\pi} \int_{-\infty}^{\infty} \frac{x(t')}{t-t'} dt', \quad (12)$$

where the integral is the Cauchy principal value integral. It yields

$$z(t) = x(t) + i\tilde{x}(t), \quad (13)$$

which is called the analytic signal of $x(t)$. Thus, the instantaneous phase can be determined as follows:

$$\phi(t) = \arctan \left(\frac{\tilde{x}(t)}{x(t)} \right). \quad (14)$$

In this paper, the EEG signal was Butterworth bandpass filtered within $\hat{f}h \pm 2$ Hz before applying the HT.

C. Discrete Fourier transform

The initial phase at a certain frequency can be also extracted using DFT with a window function and a time series data of phase components can be derived by sliding the window with a small shift size similarly to the short-time Fourier transform. The DFT of a signal $x(n)$ is defined as

$$F(k) = \sum_{n=0}^{N-1} x(n) e^{-i\frac{2\pi nk}{N}}, \quad (15)$$

where n is the sample point. The instantaneous phase can be derived as follows:

$$\phi(t) = \arctan \left(\frac{\Im(F(k))}{\Re(F(k))} \right). \quad (16)$$

Here, we set a length of the sliding window as 1.0 second and the step size was one sample.

2.4. Contrast method

Xia *et al.* proposed a method [5] to discriminate between the IC and the NC state using the canonical correlation coefficients derived from CCA. In the IC state, the correlation coefficient corresponding to the stimulus frequency is expected to be the largest while the other correlation coefficients are small. On the other hand, in the NC state, the correlation coefficients are not different each other significantly. Under this assumption, a threshold was set to distinguish the IC state from the NC state as follows:

$$\frac{\rho_{\text{sec}}}{\rho_{\text{max}}} \leq \theta, \quad (17)$$

Table 2. Comparative results of the sensitivity (SEN) and the specificity (SPC). In the table, CWT, HT, and DFT stand for continuous wavelet transform, Hilbert transform, and discrete Fourier transform, respectively.

Subject	Proposed method						Xia <i>et al.</i> 's method	
	CWT		HT		DFT		SEN [%]	SPC [%]
	SEN [%]	SPC [%]	SEN [%]	SPC [%]	SEN [%]	SPC [%]	SEN [%]	SPC [%]
sub1	74	84	70	82	68	84	60	76
sub2	40	82	42	72	50	72	54	40
sub3	82	82	70	88	70	80	70	82
sub4	60	78	58	72	62	78	56	82
sub5	62	90	58	74	54	72	46	84
sub6	50	74	46	76	40	72	44	74
Mean	61.2	81.7	57.3	77.3	57.3	76.3	55.0	73.0
S.D.	0.15	0.05	0.12	0.06	0.12	0.05	0.10	0.17

where ρ_{\max} is the largest correlation coefficient and ρ_{sec} is the second largest correlation coefficient. The threshold θ for each subject was manually set according to their performance in the synchronous experiment. In this paper, we chose the threshold θ according to the Bayesian classification rule. It set the threshold θ where the posterior probability of the IC state was equal to that of the NC state.

2.5. Performance evaluation

To evaluate the performance of the proposed method, we used sensitivity and specificity defined as follows:

$$\text{SEN} = \frac{\text{TP}}{\text{TP} + \text{FN}}, \quad (18)$$

$$\text{SPC} = \frac{\text{TN}}{\text{FP} + \text{TN}}, \quad (19)$$

where TP (true positive) and FN (false negative) occur in the IC state while FP (false positive) and TN (true negative) occur in the NC state. Thus SEN = 100 % means that all the IC states are correctly detected and SPC = 100 % does that all the NC states are correctly detected. Moreover, we measured the command recognition accuracy under the condition of TP.

3. RESULTS AND DISCUSSIONS

The performance was evaluated based on the leave-one-out cross-validation. Table 2 shows the comparative results of the sensitivity and the specificity of the proposed method using the CWT, the HT and the DFT, and Xia *et al.*'s method.

The proposed method showed better performance than Xia *et al.*'s method in both of the sensitivity and the specificity. In Xia *et al.*'s method, the sensitivity and the specificity of sub2 were both lower than the proposed method. It seemed that sub2 had weak responses of the SSVEP, which made the ratio of rho defined in (17) in the IC state not greater enough than that in the NC state. It suggests that Xia *et al.*'s method is not suitable to discriminate IC/NC states for a user whose responses of the SSVEP are not very strong. On the contrary, it seems that the proposed method has robustness even for such a user. In terms of phase detection in the proposed method, the CWT showed better performance than the other two methods in the sensitivity and the specificity.

Across all three methods, the specificities were higher than the sensitivities. This result seems reasonable because the NC state is more frequent than the IC state in a real environment. Moreover,

Table 3. The command recognition accuracy under the condition of true positive (TP).

Subject	Accuracy [%]
sub1	97.3
sub2	85.0
sub3	97.6
sub4	93.3
sub5	87.1
sub6	88.0
Mean	91.38
S.D.	0.05

FPs are more annoying than FNs to users, i.e., they would prefer spending longer time inputting commands to allowing the BCIs to execute unintended commands.

Table 3 shows the command recognition accuracy of the proposed method when TP occurred, i.e., the IC state was detected as IC correctly. This is the result when the phase was extracted by employing the CWT. The mean command recognition accuracy across the subjects was 91.38 % and it seems in a reliable level.

4. CONCLUSION

We proposed a new method to discriminate between the IC and the NC states for asynchronous BCIs based on SSVEP. The proposed method had a two-step tree structure as follows: in the first step, a SSVEP frequency was estimated with CCA, and in the next step, the state was classified as IC or NC with a classifier using the PLVs as features.

The experimental result showed that the proposed method had better performance than the previous work in the sensitivity and the specificity. The command recognition accuracy was also in a reliable level.

Although there is still room for improvement to the proposed method in terms of the sensitivity and the specificity. It would be improved using further information of phase, e.g., in this paper, the PLVs were calculated between EEG signal and the reference signal, although, the PLVs between EEG signal from two channels could be useful as well. In the future work, the issue described above will be investigated to increase the accuracy. Also, the proposed method will be implemented as an online asynchronous BCI.

5. REFERENCES

- [1] J. Wolpaw, N. Birbaumer, D. McFarland, G. Pfurtscheller, and T. Vaughan, "Brain-computer interfaces for communication and control," *Clinical Neurophysiology*, vol. 113, no. 6, pp. 767–791, Jun. 2002.
- [2] J. Wolpaw, N. Birbaumer, W. Heetderks, D. McFarland, P. Peckham, G. Schalk, E. Donchin, L. Quatrano, C. Robinson, and T. Vaughan, "Brain-computer interface technology: A review of the first international meeting," *IEEE Trans. Rehab. Eng.*, vol. 8, no. 2, pp. 164–173, Jun. 2000.
- [3] M. Middendorf, G. McMillan, G. Calhoun, and K. Jones, "Brain-computer interfaces based on the steady-state visual-evoked response," *IEEE Trans. Rehabil. Eng.*, vol. 8, no. 2, pp. 211–4, Jun. 2000.
- [4] D. Krusienski, E. Sellers, D. McFarland, T. Vaughan, and J. Wolpaw, "Toward enhanced P300 speller performance," *J. of Neuroscience Methods*, vol. 167, no. 1, pp. 15–21, Jan. 2008.
- [5] B. Xia, X. Li, H. Xie, W. Yang, J. Li, and L. He, "Asynchronous brain-computer interface based on steady-state visual-evoked potential," *Cognitive Comput.*, vol. 5, no. 2, pp. 243–251, Jun. 2013.
- [6] H. Cecotti, "A self-paced and calibration-less SSVEP-based brain-computer interface speller," *IEEE Trans. Neural Syst. Rehab. Eng.*, vol. 18, no. 2, pp. 127–133, Apr. 2010.
- [7] S. Parini, L. Maggi, A. C. Turconi, and G. Andreoni, "A robust and self-paced BCI system based on a four class SSVEP paradigm: Algorithms and protocols for a high-transfer-rate direct brain communication," *Computational Intell. Neuroscience*, vol. 2009, Feb. 2009.
- [8] J. del R Millán and J. Mouriño, "Asynchronous BCI and local neural classifiers: An overview of the adaptive brain interface project," *IEEE Trans. Neural Syst. Rehab. Eng.*, vol. 11, no. 2, pp. 159–161, Jun. 2003.
- [9] A. A. Nooh, J. Yunus, and S. M. Daud, "A review of asynchronous electroencephalogram-based brain computer interface systems," in *Int. Conf. Biomed. Eng. Tech. IPCBEE*, vol. 11, 2011, pp. 55–59.
- [10] R. Scherer, A. Schloegl, F. Lee, H. Bischof, J. Janša, and G. Pfurtscheller, "The self-paced graz brain-computer interface: Methods and applications," *Computational Intell. Neuroscience*, vol. 2007, Jul. 2007.
- [11] P. Martinez, H. Bakardjian, and A. Cichocki, "Fully online multicommand brain-computer interface with visual neurofeedback using SSVEP paradigm," *Computational Intell. Neuroscience*, vol. 2007, p. 94561, Jan. 2007.
- [12] Y. Zhang, G. Zhou, Q. Zhao, A. Onishi, J. Jin, X. Wang, and A. Cichocki, "Multiway canonical correlation analysis for frequency components recognition in SSVEP-based BCIs," in *Neural Inform. Process.*, ser. Lecture Notes in Computer Science, B.-L. Lu, L. Zhang, and J. Kwok, Eds. Springer Berlin Heidelberg, 2011, vol. 7062, pp. 287–295.
- [13] M. Cheng, X. Gao, S. Gao, and D. Xu, "Design and implementation of a brain-computer interface with high transfer rates," *IEEE Trans. Biomed. Eng.*, vol. 49, no. 10, pp. 1181–1186, Oct. 2002.
- [14] G. Pfurtscheller, T. Solis-Escalante, R. Ortner, P. Linortner, and G. R. Muller-Putz, "Self-paced operation of an SSVEP-based orthosis with and without an imagery-based "brain switch:" a feasibility study towards a hybrid BCI," *IEEE Trans. Neural Syst. Rehab. Eng.*, vol. 18, no. 4, pp. 409–414, Aug. 2010.
- [15] G. R. Muller-Putz and G. Pfurtscheller, "Control of an electrical prosthesis with an SSVEP-based BCI," *IEEE Trans. Biomed. Eng.*, vol. 55, no. 1, pp. 361–364, Jan. 2008.
- [16] R. Leeb, D. Friedman, G. R. Müller-Putz, R. Scherer, M. Slater, and G. Pfurtscheller, "Self-paced (asynchronous) BCI control of a wheelchair in virtual environments: A case study with a tetraplegic," *Computational Intell. Neuroscience*, vol. 2007, Jul. 2007.
- [17] H. H. Jasper, "The ten twenty electrode system of the international federation," *Electroencephalography and Clinical Neurophysiology*, vol. 10, no. 2, pp. 371–375, 1958.
- [18] H. Bakardjian, T. Tanaka, and A. Cichocki, "Optimization of SSVEP brain responses with application to eight-command brain-computer interface," *Neuroscience Letters*, vol. 469, no. 1, pp. 34–38, Jan. 2010.
- [19] Y. Kimura, T. Tanaka, H. Higashi, and N. Morikawa, "SSVEP-based brain-computer interfaces using FSK-modulated visual stimuli," *IEEE Trans. Biomed. Eng.*, vol. 60, no. 10, pp. 2831–2838, Oct. 2013.
- [20] Z. Lin, C. Zhang, W. Wu, and X. Gao, "Frequency recognition based on canonical correlation analysis for SSVEP-based BCIs," *IEEE Trans. Biomed. Eng.*, vol. 53, no. 12, pp. 2610–2614, Dec. 2006.
- [21] J.-P. Lachaux, E. Rodriguez, J. Martinerie, F. J. Varela *et al.*, "Measuring phase synchrony in brain signals," *Human Brain Mapping*, vol. 8, no. 4, pp. 194–208, May 1999.
- [22] E. Gysels and P. Celka, "Phase synchronization for the recognition of mental tasks in a brain-computer interface," *IEEE Trans. Neural Syst. Rehab. Eng.*, vol. 12, no. 4, pp. 406–415, Dec. 2004.
- [23] Y. Wang, B. Hong, X. Gao, and S. Gao, "Phase synchrony measurement in motor cortex for classifying single-trial EEG during motor imagery," in *Eng. Medicine Biology Soc. (EMBC), 2006 28th Ann. Int. Conf. IEEE*, 2006, pp. 75–78.
- [24] V. J. Samar, A. Bopardikar, R. Rao, and K. Swartz, "Wavelet analysis of neuroelectric waveforms: A conceptual tutorial," *Brain and Language*, vol. 66, no. 1, pp. 7–60, Jan. 1999.
- [25] R. X. Gao and R. Yan, *Wavelets: Theory and Applications for Manufacturing*. New York: Springer, 2010.
- [26] K. Tanaka, Y. Mizuno, T. Tanaka, and K. Kitajo, "Detection of phase synchronization in EEG with bivariate empirical mode decomposition," in *Eng. Medicine Biology Soc. (EMBC), 2013 35th Ann. Int. Conf. IEEE*, 2013, pp. 973–976.
- [27] C. Tallon-Baudry, O. Bertrand, C. Delpuech, and J. Pernier, "Stimulus specificity of phase-locked and non-phase-locked 40 Hz visual responses in human," *J. of Neuroscience*, vol. 16, no. 13, pp. 4240–4249, Jul. 1996.
- [28] S. L. Hahn, *Hilbert Transforms in Signal Processing*. London: Artech House, 1996.